Tension Line Fields in a Simply Supported Blanket Subjected to In-Plane Body Forces

Fred Rimrott* and Blair Kingsland†
University of Toronto, Toronto, Canada

Recent renewed interest in tension field theory is due to the intended use of large plastic blankets as load-carrying substrate for solar power collection arrays. Such substrate are used on spacecraft that extend their solar panels on the transfer orbit from low-Earth orbit to geosynchronous orbit, and are consequently subjected to acceleration during apogee engine firing, with the inertial force's component in the plane of the blanket leading to the formation of wrinkles. The present paper contains a fundamental study, with experiments, of the wrinkling patterns of a simply supported blanket of uniform thickness, pretensioned in longitudinal direction, and subject to uniform loading in transverse direction.

Nomenclature

T = pretension, N
T_1 = pretension of primary field, N
T_2 = pretension of secondary field, N
W = uniformly distributed body force (load), N
W_1 = portion of W in primary field
W_2 = portion of W in secondary field
g = 9.80665 m/s^2
h = blanket height, m
h_1 = height of primary field at blanket center, m
h_2 = height of secondary field at blanket center, m
h_p = height of primary field anywhere in blanket, m
h_s = height of secondary field anywhere in blanket, m
l = blanket length, m
q = body force (load) per unit length, N/m
s = visible sag at blanket center, m
s' = sag of centerline of secondary field, m
α = angle between x- and η-direction
α_p = angle of top tension line in primary field
α_s = angle of bottom tension line in secondary field
θ = inclination angle of blanket end bars
ρ = blanket material density, kg/m^3
σ = tensile stress, Pa
τ = shear stress, Pa

Introduction

THE recent upsurge of interest in tension field theory has come about by the intended use of large plastics blankets of, say, 3 m width and 10 m length, as load-carrying substrate for solar power collection arrays, on spacecraft that extend their solar arrays fully or partially on the transfer orbit from low-Earth orbit to geosynchronous orbit. During firing of the apogee engine the blankets are subjected to acceleration producing an inertial force with components in, and normal to, the plane of the blankets. It is the in-plane component that has been given inadequate attention in the past. It is troublesome because it leads to wrinkling.

Fortunately, in-plane loading can easily be simulated under laboratory conditions on the surface of the Earth by using the blanket's weight as body force, plus scaling and/or additional uniformly distributed weight wafers attached to the blanket, if necessary. By laboratory tests and accompanying analyses, fundamental loading cases can thus be studied readily.

Received Oct. 27, 1982; revision received March 15, 1984.

*Professor, Department of Mechanical Engineering.
†Graduate Student, Department of Mechanical Engineering.

The treatment of in-plane loading of thin plates begins with Wagner's[1] papers; the terms tension field theory and tension line enter the picture with Reissner's[2] work. Stein and Hedgepeth[3] introduce the variable Poisson ratio, and Mansfield[4] the term tension ray, instead of tension line.

The term tension ray emphasizes a conclusion reached by every investigator, namely that tension lines, and wrinkles for that matter, are straight. This, however, need not be the case. As a matter of fact, it is not the case when body forces are considered,[5] as is the case in the present investigation. Experimental evidence for the case of a simply supported blanket (Fig. 1) points to the presence of two tension line fields, the primary tension line field in the lower portion of the blanket, and the secondary tension line field, which, as will be shown, grows from zero size at zero load to assume more and more of the load as it increases, at the expense of the primary tension line field which eventually vanishes altogether.

The present problem belongs to a class, where the blanket is pretensioned by a constant tension force T in horizontal direction. There are two rigid bars at the ends $x = \pm l/2$ of the blanket. The blanket is loaded vertically by a uniformly distributed body force W in negative y-direction. The boundaries $y = 0$ and $y = h$ of the blanket are free.

Blanket Theory

Equilibrium on a blanket element (Fig. 1) leads to a differential equation

$$\frac{d^2y}{dx^2} = \frac{q}{T} \tag{1}$$

which governs the shape $y = y(x)$ of tension lines in the presence of body forces q in y-direction and a pretension force T in x-direction.

The blanket and its loading obviously represent a plane stress case, for which the equilibrium equations for the stress components in the blanket are

$$\frac{\partial \sigma_x}{\partial x} + \frac{\partial \tau_{xy}}{\partial y} = 0$$
$$\frac{\partial \sigma_y}{\partial y} + \frac{\partial \tau_{xy}}{\partial x} = \rho g \tag{2}$$

where ρ is the material density and g the gravitational attraction constant.

Following, e.g., Stein and Hedgepeth,[3] we set two principal stresses to zero

$$\sigma_\xi = \sigma_\zeta = 0$$

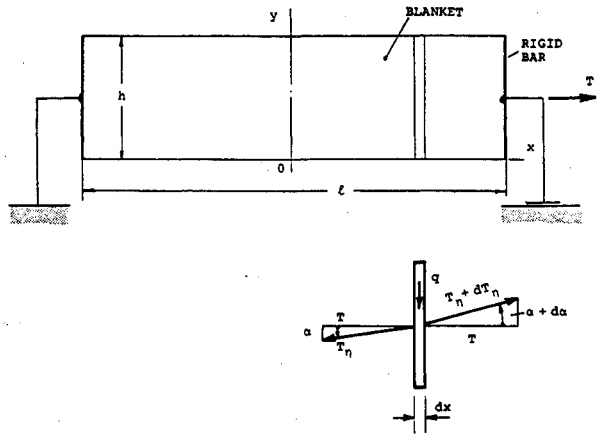

Fig. 1 Simply supported uniform blanket with pretension.

The stress components in an xy-coordinate system in the plane of the blanket are then

$$\sigma_x\sigma_y = \tau_{xy}^2$$

$$\sigma_x = \sigma_\eta \cos^2\alpha$$

$$\sigma_y = \sigma_\eta \sin^2\alpha$$

$$\tau_{xy} = \sigma_\eta \sin\alpha\cos\alpha \tag{3}$$

where α is the angle between the x-axis and the η-principal stress axis (Fig. 2).

Primary Tension Line Field

The primary tension line field carries a body force per unit length of

$$q = \frac{W}{l}\frac{y}{h} \tag{4}$$

such that the tension line equation (1) becomes for the primary field (Fig. 2)

$$\frac{d^2y}{dx^2} - \frac{W}{T_1 hl}y = 0 \tag{5}$$

Observing the boundary conditions, $y = h_1$ and $dy/dx = 0$ when $x = 0$, the solution of Eq. (3) is

$$y = h_1 \cosh\sqrt{\frac{W}{T_1 lh}}\,x \tag{6}$$

and represents the top tension line. The equation for any other tension line in the primary field is

$$y = c_1 h_1 \cosh\sqrt{\frac{W}{T_1 lh}}\,x \tag{7}$$

with

$$0 \le c_1 < 1 \tag{8}$$

For the top tension line, it is convenient to introduce a new symbol h_p (Fig. 2), such that Eq. (6) now reads

$$h_p = h_1 \cosh\sqrt{\frac{W}{T_1 lh}}\,x \tag{9}$$

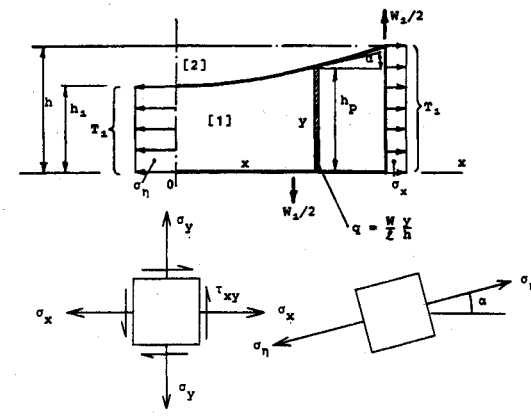

Fig. 2 Primary tension line field and stress on blanket elements.

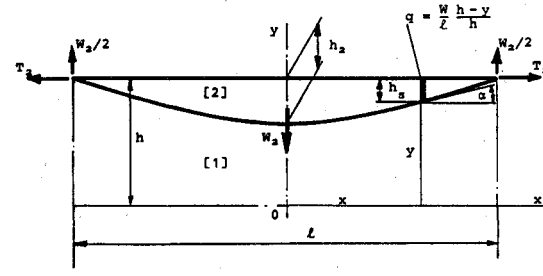

Fig. 3 Secondary tension line field.

When $x = l/2$ the top tension line reaches $h_p = h$, and consequently

$$h_1 = \frac{h}{\cosh\sqrt{\dfrac{Wl}{4T_1 h}}} \tag{10}$$

Secondary Tension Line Field

An inspection of Fig. 3 indicates that the secondary field carries a body force of

$$q = \frac{W}{l}\frac{h-y}{h} \tag{11}$$

such that the tension line equation (1) becomes for the secondary field

$$\frac{d^2y}{dx^2} + \frac{W}{T_2 hl}y = \frac{W}{T_2 l} \tag{12}$$

With appropriate boundary conditions, the solution of Eq. (12) is

$$y = h - h_2 \cos\sqrt{\frac{W}{T_2 hl}}\,x \tag{13}$$

which represents the bottom tension line of the secondary field. For convenience, we introduce h_s for this line (Fig. 3) and write

$$h_s = h_2 \cos\sqrt{\frac{W}{T_2 hl}}\,x \tag{14}$$

The secondary tension line field is a family of cosine curves.

Any other tension line in the secondary field is given by

$$y = h - c_2 h_2 \cos\sqrt{\frac{W}{T_2 h l}}\, x \tag{15}$$

with $0 \le c_2 < 1$.

The secondary field facilitates a determination of the horizontal component of its tension force. Since $h_s = 0$ when $x = l/2$, Eq. (14) provides us with

$$\sqrt{\frac{W}{T_2 h l}}\,\frac{l}{2} = \frac{\pi}{2} \tag{16}$$

or

$$T_2 = \frac{Wl}{\pi^2 h} \tag{17}$$

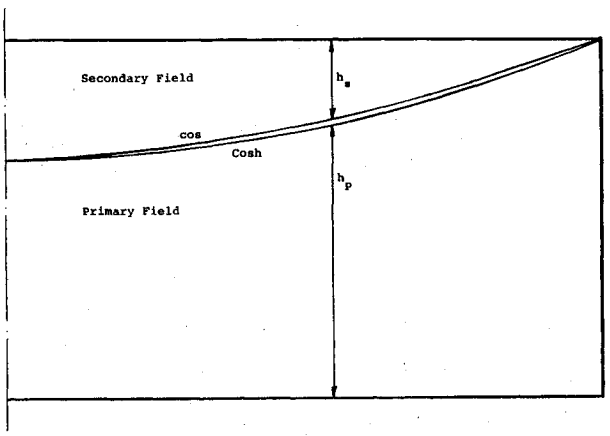

Fig. 4 Interface between primary and secondary tension line field.

Table 1 Cosh and cos functions along interface

	$h_p = \dfrac{h}{\cosh\sqrt{\frac{Wl}{4T_1 h}}}\cosh\sqrt{\frac{Wl}{4T_1 h}}\,\frac{2x}{l}$	$h - h_s = h - h_2\cos\frac{\pi}{l}x$
x/l	m	m
0	2	2
0.1	2.037 1649	2.048 9435
0.2	2.150 0409	2.190 9830
0.3	2.342 8229	2.412 2147
0.4	2.622 6757	2.690 9830
0.5	3	3

Thus the horizontal tension force component of the secondary tension field system is directly proportional to the in-plane load (Fig. 4) and independent of the pretension T.

In order to retain the "simple" supports (Fig. 1), the applied tension force T, the primary field tension force T_1, and the secondary field tension force T_2 must be related by

$$T = T_1 + 2T_2 \tag{18}$$

With the help of Eqs. (17) and (18) the primary field tension force can now be expressed in terms of the total pretension force T and the applied load W

$$T_1 = T - \frac{2l}{\pi^2 h} W \tag{19}$$

Knowing T_2, Eq. (14) can now be more simply expressed as (Table 1 and Fig. 4)

$$h_s = h_2 \cos\frac{\pi}{l} x \tag{20}$$

Equation (19) may also be entered into Eq. (10) to give the height of the primary region

$$h_1 = \frac{h}{\cosh\sqrt{\dfrac{\pi^2 Wl}{4(\pi^2 Th - 2Wl)}}} \tag{21}$$

An inspection of Eq. (21) indicates that when there is no load, i.e., when $W = 0$, then $h_1 = h$, i.e., the primary region covers the entire blanket. As the load increases, the secondary field begins to form, and becomes larger and larger. Eventually, the primary region's height at the blanket's center vanishes, i.e., $h_1 = 0$, when the load has reached a value of $W = \pi^2 Th/2l$. For this condition, the primary tension force $T_1 = 0$, i.e., the primary field has vanished altogether.

Since always

$$h = h_1 + h_2$$

the height h_2 of the secondary field at the blanket center becomes (Table 2 and Fig. 5)

$$h_2 = h\left(1 - \operatorname{sech}\sqrt{\frac{\pi^2 Wl}{4(\pi^2 Th - 2Wl)}}\right) \tag{22}$$

Table 2 Parameters as function of applied load W for a blanket of height $h = 3$ m, length $l = 10$ m, and pretension $T = 60$ N

Body force W, N	Ratio W/T	Pretension T_2, N	Pretension T_1, N	Height h_2, m	Ratio h_2/h_1	Height h_1, m	Sag s, m	Angle θ, deg	Stress at $x=0$ T_2/h_2, N/m	T_1/h_1, N/m	Body Force W_2, N	Body Force W_1, N	Ratio W_2/W	Ratio W_1/W
0	0	0	60	0	0	3	0	0	16.211[c]	20	0	0	0	1
10	0.167	3.377	53.246	0.220	0.079	2.780	0.114	0.031	15.350	19.153	0.991	0.009	0.099	0.901
20	0.333	6.755	46.490	0.467	0.185	2.533	0.253	0.151	14.465	18.354	1.982	18.018	0.099	0.901
30	0.5	10.132	39.736	0.746	0.331	2.254	0.426	0.428	13.582	17.629	4.749	25.251	0.158	0.842
40	0.667	13.509	32.982	1.064	0.550	1.936	0.647	0.986	12.696	17.036	9.032	30.968	0.226	0.774
50	0.833	16.887	26.226	1.425	0.905	1.575	0.934	2.055	11.851	16.651	15.120	34.880	0.302	0.698
60	1.000	20.264	19.472	1.839	1.584	1.161	1.326	4.143	11.019	16.772	23.415	36.585	0.390	0.610
70	1.167	23.642	12.716	2.305	3.316	0.695	1.871	8.248	10.257	18.296	34.240	35.760	0.492	0.512
80	1.333	27.019	5.962	2.788	13.151	0.212	2.604	15.977	9.690	28.123	47.331	32.669	0.592	0.408
88.826[a]	1.480[b]	30	0	3	∞	0	3	21.206	10	∞	56.548[d]	32.278	0.637	0.363

[a] $= \frac{\pi^2}{2}\frac{h}{l}T$ [b] $= \frac{\pi^2 h}{2l}$ [c] $= \frac{8T}{\pi^2 h}$ [d] $= \frac{2}{\pi}W$

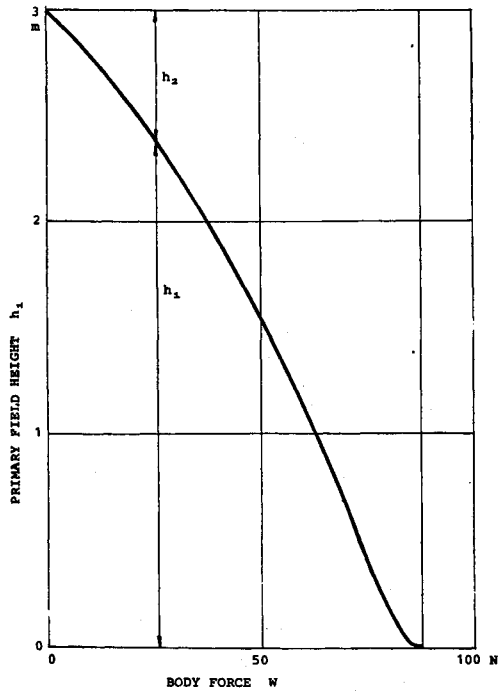

Fig. 5 Field heights vs load.

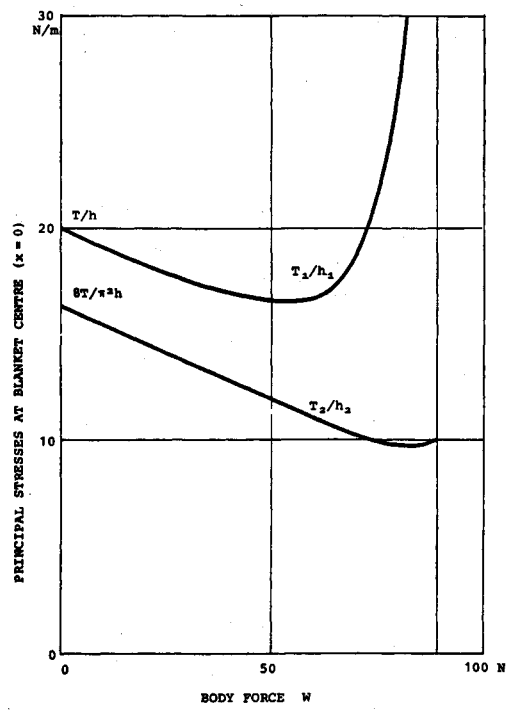

Fig. 6 Principal stress at blanket center ($x = 0$) vs load.

and furthermore

$$\frac{h_2}{h_1} = \cosh\sqrt{\frac{\pi^2 Wl}{4(\pi^2 Th - 2Wl)}} - 1 \tag{23}$$

Stresses in Primary Tension Line Field

The stress components in xy-coordinates for any point (x, y) within the primary field are, from Eq. (3),

$$\sigma_x = \frac{T_1}{bh_p} = \frac{T_1}{bh_1 \cosh\sqrt{\frac{W}{T_1 hl}}\, x} \tag{24}$$

$$\sigma_y = \frac{Wy^2}{bh_1 hl} \frac{\tanh^2\sqrt{\frac{W}{T_1 hl}}\, x}{\cosh\sqrt{\frac{W}{T_1 hl}}\, x} \tag{25}$$

$$\tau_{xy} = \frac{T_1 y}{bh_1} \frac{W}{T_1 hl} \frac{\tanh\sqrt{\frac{W}{T_1 hl}}\, x}{\cosh\sqrt{\frac{W}{T_1 hl}}\, x} \tag{26}$$

The principal stresses are

$$\sigma_\eta = \frac{T_1}{bh_1 \cosh\sqrt{\frac{W}{T_1 hl}}\, x}\left(1 + \frac{Wy^2}{T_1 hl}\tanh^2\sqrt{\frac{W}{T_1 hl}}\, x\right)$$

$$\sigma_\xi = \sigma_\zeta = 0 \tag{27}$$

The angle α between the principal stress σ_η and the x-axis can be obtained from

$$\tan\alpha = \sqrt{\frac{W}{T_1 hl}}\, y \tanh\sqrt{\frac{W}{T_1 hl}}\, x \tag{28}$$

The slope of the top tension line in the primary field at the built-in end ($y = h$, $x = l/2$) is

$$\tan\alpha_p = \sqrt{\frac{W}{T_1 hl}}\, h \tanh\sqrt{\frac{Wl}{4T_1 h}} \tag{29}$$

At the blanket's line of symmetry, $x = 0$ and

$$(\sigma_x)_{x=0} = (\sigma_\eta)_{x=0} = \frac{T_1}{bh_1} \tag{30}$$

With the help of Eqs. (19) and (21), the ratio T_1/h_1 at the blanket's line of symmetry can be written

$$\frac{T_1}{h_1} = \frac{\pi^2 Th - 2Wl}{\pi^2 h^2 \operatorname{sech}\sqrt{\frac{\pi^2 Wl}{4(\pi^2 Th - 2Wl)}}} \tag{31}$$

See Figs. 5 and 6.

Stresses in Secondary Tension Line Field

Using xy-coordinates, the stress components in the secondary tension line field are, from Eq. (3),

$$\sigma_x = \frac{T_2}{bh_s} = \frac{T_2}{bh_2 \cos\sqrt{\frac{W}{T_2 hl}}\, x} \tag{32}$$

$$\sigma_y = \frac{Wy^2}{bh_2 hl} \frac{\tan^2\sqrt{\frac{W}{T_2 hl}}\, x}{\cos\sqrt{\frac{W}{T_2 hl}}\, x} \tag{33}$$

$$\tau_{xy} = \frac{T_2(h-y)}{bh_2}\sqrt{\frac{W}{T_2 hl}} \tan\sqrt{\frac{W}{T_2 hl}}\, x \tag{34}$$

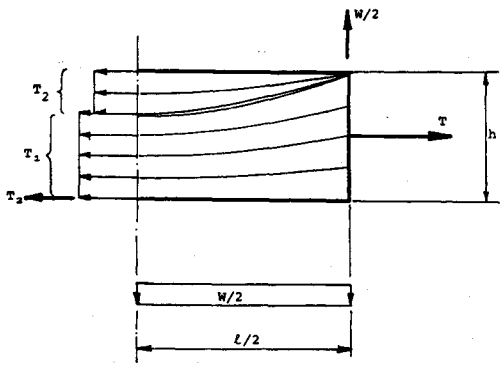

Fig. 7 Principal stress distribution at blanket center ($x = 0$).

The principal stresses are

$$\sigma_\eta = \frac{T_2}{bh_2 \cos\sqrt{\frac{W}{T_2 hl}}\,x}\left(1 + \frac{W(h-y)^2}{T_2 hl}\tan^2\sqrt{\frac{W}{T_2 hl}}\,x\right)$$

$$\sigma_\xi = \sigma_\zeta = 0 \tag{35}$$

The tangent of the angle α between the first principal stress direction and the x-axis is

$$\tan\alpha = \sqrt{\frac{W}{T_2 hl}}\,(h-y)\tan\sqrt{\frac{W}{T_2 hl}}\,x \tag{36}$$

or, since $T_2 = Wl/\pi^2 h$

$$\tan\alpha = \frac{\pi}{l}(h-y)\tan\frac{\pi}{l}x \tag{37}$$

The slope of the h_s line at the built-in end, which is of finite magnitude, can be obtained by introducing h_s from Eq. (19),

$$\tan\alpha_s = \frac{\pi}{l}h_2\cos\frac{\pi}{l}x\tan\frac{\pi}{l}x = \frac{\pi}{l}h_2\sin\frac{\pi}{l}x \tag{38}$$

when $x = l/2$, then

$$\tan\alpha_s = \frac{\pi}{l}h_2 \tag{39}$$

At the blanket's line of symmetry, $x = 0$, and consequently

$$(\sigma_x)_{x=0} = (\sigma_\eta)_{x=0} = \frac{T_2}{bh_2} \tag{40}$$

(See Fig. 7.) With the help of Eqs. (10), (17), and (22), the ratio T_2/h_2 at the blanket's line of symmetry can be written

$$\frac{T_2}{h_2} = \frac{Wl}{\pi^2 h^2\left(1 - \operatorname{sech}\sqrt{\frac{\pi^2 Wl}{4(\pi^2 Th - 2Wl)}}\right)} \tag{41}$$

See also Figs. 5 and 6.

Sag

As the load W increases while the pretension T remains constant, the secondary tension line field grows larger and larger. Its height h_2 at the center ($x = 0$) increases according to Eq. (22), which is plotted in Fig. 5.

The tension line theory and the solution proposed in the present paper are based on the assumption that the blanket geometry remains unchanged. This is, of course, not the case and the most pronounced geometry change is the sag (Fig. 8) of the topmost fiber. In contradistinction, the bottommost fiber remains essentially straight. After all, it carries a concentrated force T_2, which, furthermore, increases as the load W increases.

If one considers that portion of the blanket which contains the secondary tension line field is sagging like a cable subjected to a load that is equal to the weight/length of the secondary tension line field, i.e.,

$$q = \frac{W}{l}\frac{h_s}{h} = \frac{W}{lh}h_2\cos\frac{\pi}{l}x \tag{42}$$

then the shape of the catenary (Fig. 8) is obtained from

$$\frac{d^2y}{dx^2} = \frac{q}{T_2} = \frac{W}{T_2 lh}h_2\cos\frac{\pi}{l}x \tag{43}$$

which when all applicable boundary conditions are observed gives

$$y = h - h_2\cos\frac{\pi}{l}x \tag{44}$$

When $x = 0$, then

$$y = h - s' \tag{45}$$

giving

$$s' = h_2 \tag{46}$$

The sag s' is, however, not the visible sag s (Fig. 8) that can readily be measured. In order to obtain s, we assume uniform wrinkling along $x = 0$, such that

$$s' = s + \frac{h-s}{2h}h_2 \tag{47}$$

and with $s' = h_2$ from Eq. (46), the visible sag s becomes

$$s = \frac{hh_2}{2h - h_2} \tag{48}$$

In Fig. 9, the visible sag is plotted against the applied load W. The slope angle θ of the rigid end bars is related to the visible sag and can be obtained by assuming that the blanket length l remains constant (Fig. 8).

For small angles θ, each end can be shown to move in by an amount (Fig. 8)

$$\frac{\pi^2}{8}\frac{s^2}{l} \tag{49}$$

such that

$$\theta = \frac{\pi^2}{8}\frac{s^2}{hl} \tag{50}$$

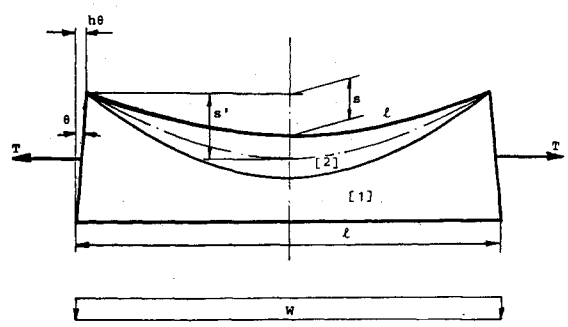

Fig. 8 Sag s' of secondary field and visible sag s.

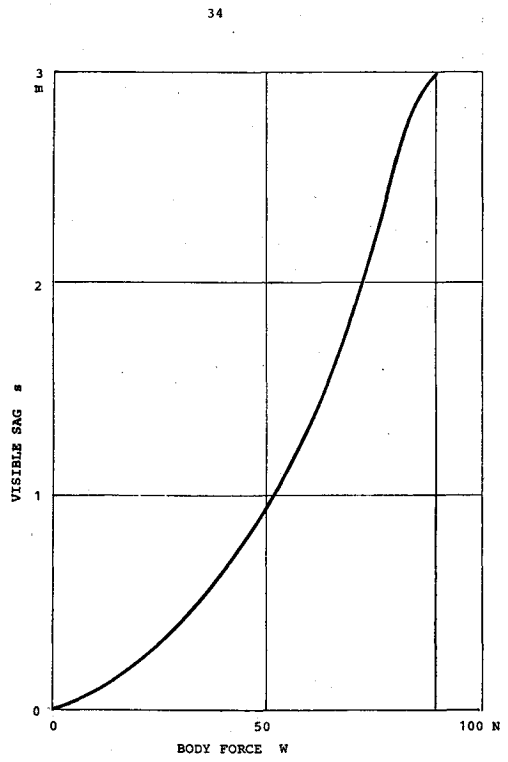

Fig. 9 Visible sag vs load.

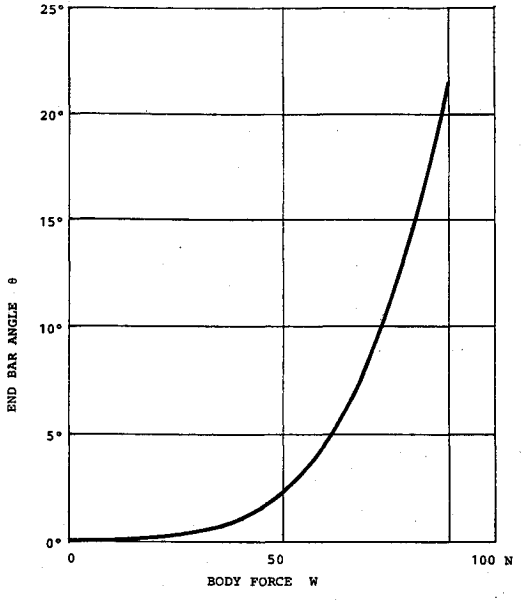

Fig. 10 End bar angle vs load.

A plot of slope angle θ vs applied load W is given in Fig. 10.

Interface

The interface between primary and secondary tension line field is at

$$h_s = h_2 \cos\frac{\pi}{l} x \tag{51}$$

and at

$$h_p = h_1 \cosh\sqrt{\frac{W}{T_1 lh}}\, x \tag{52}$$

Ideally, these two should coincide. In reality, they differ by a small amount, as shown in Fig. 4. Considering the wrinkling, the blanket should readily be able to accommodate this discrepancy. By close inspection of Fig. 11, the cos shape of one wrinkle can indeed be made out, vs the cosh shape of the neighboring wrinkle.

At the interface between primary and secondary fields there is no stress transmitted, i.e.,

$$\sigma_\xi = \tau_{\xi\eta} = 0 \tag{53}$$

There is, on the other hand, a stress discontinuity in the principal stress component along the tension lines.

The principal stress σ_η jumps from

$$\frac{T_1}{bh_p}\left(1 + \frac{Wh_p^2}{T_1 hl}\tanh^2\sqrt{\frac{W}{T_1 hl}}\, x\right) \tag{54}$$

in the primary region to

$$\frac{T_2}{bh_s}\left(1 + \frac{Wh_s^2}{T_2 hl}\tan^2\sqrt{\frac{W}{T_2 hl}}\, x\right) \tag{55}$$

in the secondary region (Figs. 7 and 12). There is a step change in σ_η at the interface between primary and secondary tension line fields (Figs. 7 and 12). If the blanket material is assumed inextensible, such a step increase across the boundary is permissible.

The secondary tension line field carries a portion W_2 of the total body force W, which can be obtained from

$$W_2 = 2\frac{W}{hl}\int_0^{l/2} h_s \, dx \tag{56}$$

With h_s from Eq. (20)

$$W_2 = \frac{2}{\pi}\frac{h_2}{h} W \tag{57}$$

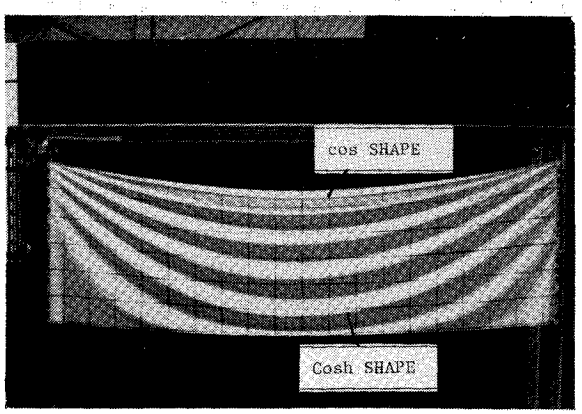

Fig. 11 Experimental blanket.

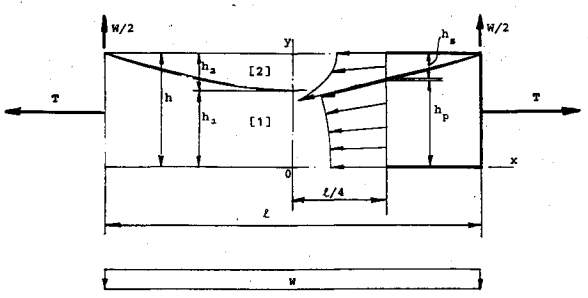

Fig. 12 Principal stress distribution at $x = l/4$.

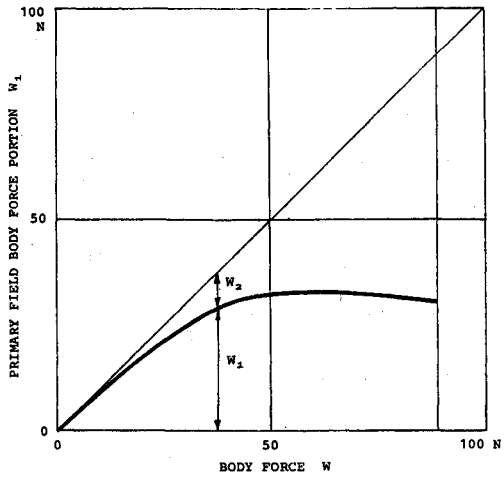

Fig. 13 Load portions carried by each field vs load.

and with h_2 from Eq. (22)

$$W_2 = \frac{2}{\pi} W\left(1 - \operatorname{sech}\sqrt{\frac{\pi^2 Wl}{4(\pi^2 Th - 2Wl)}}\right) \tag{58}$$

The primary tension line field carries a portion W_1 of the total body force W, which can either be obtained from

$$W_1 = 2\frac{W}{hl}\int_0^{l/2} h_p \, dx \tag{59}$$

or by using

$$W_1 = W - W_2 \tag{60}$$

which with the help of Eq. (58) becomes

$$W_1 = W\left(1 - \frac{2}{\pi}\left(1 - \operatorname{sech}\sqrt{\frac{\pi^2 Wl}{4(\pi^2 Th - 2Wl)}}\right)\right) \tag{61}$$

When solved, Eq. (59) gives a slightly smaller value for W_1 than Eq. (61) which includes the weight of the narrow interface strip $h - h_p - h_s$ (Fig. 4). The portions W_1 and W_2 of the body force W are plotted in Fig. 13 as function of the body force applied.

A study of Fig. 13 indicates that, as the load approaches $s\pi^2 hT/2l$, the present solution becomes progressively less accurate. The present solution, for example, predicts that as the load W approaches $\pi^2 hT/2l$ the primary field disappears completely (i.e., $T_1 = 0$), and yet it still carries a load of $(1 - 2/\pi)W$. In reality, a tertiary field has already formed, carrying the $(1 - 2/\pi)W$ and transferring it to the secondary field, which thus loses its pure cosine shape.

Diagrams

All diagrams and sample calculations are for a simply supported blanket of l = length, 10 m, h = height, 3 m, and T = pretension, 60 N, for values of the applied load from zero to $\pi^2 hT/2l = 88.826$ N, at which level the primary tension line field has just vanished ($h_1 = T_1 = 0$). Approaching this load, the theory becomes less and less accurate. Beyond this load, the two tension line fields used in the present analysis no longer exist, for all intents and purposes. Furthermore, the blanket sag has reached a level by then which indicates that geometric changes have reached magnitudes that can no longer be ignored.

Figure 11 shows a simply supported blanket of 3 m length and 0.9 m height at a load level $W/T = 0.642$ during an experiment,[3] and Figs. 14 and 15 show the same kind of blanket at various load levels.

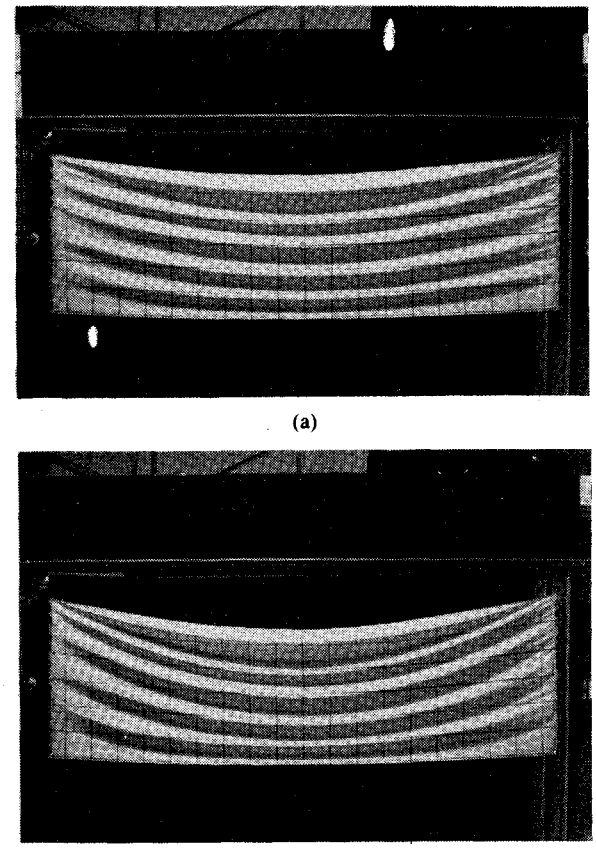

(a) (b)

Fig. 14 Experimental wrinkle patterns: a) $W/T = 0.44$; b) $W/T = 0.64$.

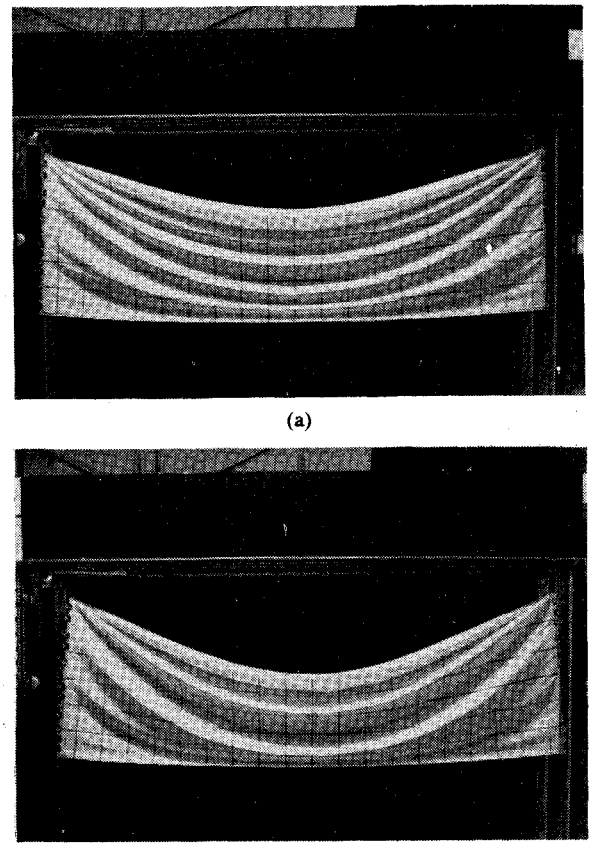

(a) (b)

Fig. 15 Experimental wrinkle patterns: a) $W/T = 0.90$; b) $W/T = 1.12$.

Conclusion

The paper shows that as the in-plane loading of a blanket commences, a primary tension line field forms first, which consists of tension lines of hyperbolic cosine shape which cover the whole blanket at the limiting case of zero load. The secondary field, which consists of tension lines of trigonometric cosine shape, begins to form as soon as the loading increases. It becomes larger at the expense of the primary field, with increasing load, until a load of $W=\pi^2Th/2l$ has been reached, at which the tension portion T_l carried by the primary field has become 0.

In view of Mansfield's admonition, "Instead, the approximate nature of tension field theory itself does not justify too scrupulous an attention to detail",[4] the equations presented in this paper provide a surprisingly accurate representation of the stress and deformation state and give excellent predictions as long as the load is very small, say up to $W/T=\frac{1}{2}(\pi^2h/2l)$, and good predictions for larger loads up to, say, $W/T=\pi^2 2h/2l$.

Acknowledgments

The authors would like to thank Spar Aerospace Limited for bringing the problem class to their attention, and the Natural Sciences and Engineering Research Council of Canada for financial support.

References

[1]Wagner, H., "Ebene Blechwandträger mit sehr dünnem Stegblech," *Zeitschrift für Flugtechnik and Motorluftschiffahrt*, 20, (1929), 8, 200-207; 9, 227-233, 10, 256-262; 11, 279-284; 12, 306-314.

[2]Reissner, E., "On Tension Field Theory," *Proceedings of the 5th International Congress on Applied Mechanics*, 1938, 88-92.

[3]Stein, M. and Hedgepeth, J.M., "Analysis of Partly Wrinkled Membranes," NASA TN-D-813, 1961.

[4]Mansfield, E.W., "Tension Field Theory," in *Applied Mechanics*, M. Hetenyi and W. G. Vincenti, editors, Springer-Verlag, Heidelberg, 1969, pp. 305-320.

[5]Kingsland, B., "In-plane Loading of Blankets," M.A.Sc. Thesis, University of Toronto, Toronto, Can., 1983, pp. 13-30.